Sustainable Energy Technologies and Assessments 91 (2026) 105105

Contents lists available at ScienceDirect

Sustainable Energy Technologies and Assessments

journal homepage: www.elsevier.com/locate/seta

Original article

A theoretical investigation of the fuel cell efficiency on the lithium battery recharging using different fuel types

J.I. Ahuir-Torres [a,*], O. Yuksel [a,b], E. Blanco-Davis [a,*], G.V. Shagar [a], D. Hitchmough [a], J. Wang [a]

[a] Liverpool Logistics Offshore and Marine Research Institute, Liverpool John Moores University, Byrom Street, L3 3AF Liverpool, United Kingdom
[b] Marine Engineering Department, Zonguldak Bulent Ecevit University, Kepez District, Haci Eyup Street, No:1, 67300 Kdz Eregli, Zonguldak, Türkiye

ARTICLE INFO

Keywords:
Ship electrification
Renewable energies
Lithium-battery
Fuel cells
Fuel type

ABSTRACT

The International Maritime Organization (IMO) aims to reduce greenhouse gas emissions to net-zero by 2050. Batteries and fuel cells have emerged as promising technologies to meet this ambitious target in marine transport applications. Although batteries and fuel cells for marine transport applications have been studied, limited attention has been paid to the fuel-cell efficiency for battery recharging as a function of fuel type. The study theoretically examines the effect of fuel type on lithium battery recharging efficiency. A model was developed to assess battery recharging processes using fuel cells with different fuels. The model was created using the MATLAB Simulink environment. Simulations were conducted under several scenarios, including a system comprising single- and multi-type fuel cells. The results indicate that the configuration consisting of a single methanol fuel cell exhibited the highest recharging efficiency, followed by the hydrogen fuel cell configuration. Scenarios involving configurations with multiple fuel cell types exhibited lower recharging efficiency than those with a single fuel cell type, except for the ammonia fuel cell. The lowest recharging efficiency was observed in the configuration incorporating three types of fuel cells.

Introduction

The marine transport sector accounts for 3% of global greenhouse gas emissions. For this reason, the International Maritime Organization aims to reduce emissions from marine transport to achieve net zero by 2050 [1–3]. To achieve this goal, the marine transport industry is investigating multiple renewable energy alternatives, including superconductors, solar cells, wind turbines, batteries and fuel cells [4,5]. The combination of these two options has emerged as a valuable technology for reducing greenhouse gas emissions. This interest is attributed to their favourable properties, including the possibility of achieving net-zero emissions, high efficiency in power supply, and current accessibility [2,6,7]. A fuel cell typically serves as a power source for charging or recharging batteries, while the battery, in turn, provides energy to meet the marine vessel's demands. However, before incorporating this technology into marine transport applications, theoretical studies must be conducted to assess its viability and determine optimal conditions.

Lithium battery modelling has been extensively investigated in the literature. Saxena et al. [8] developed a numerical model to study the effects of state of charge (SOC) and state of health (SOH) on the power supply efficiency of lithium batteries. They determined that the decrease in the SOC difference between the recharging and discharging processes reduced battery degradation. Sepasi et al. [9] employed and developed the Coulomb-continuing method to evaluate the effects of SOC and SOH on battery performance. This method resulted in a significant reduction in computational time and source requirements for predicting battery performance. Kumar et al. [10] further, designed an accurate predictive model to investigate the influence of SOC and SOH on battery efficiency and service life for automotive applications. They utilised electrochemical, thermodynamic, and experimental data to develop this model. This model enabled the identification of optimal operational conditions to improve battery efficiency and lifespan across various operating scenarios. Chatterjee et al. [11] developed a model to monitor the efficiency and performance of a lithium-battery-powered vehicle, accounting for the influence of battery SOC and temperature on vehicle propulsion efficiency. The predictive model was developed using the MATLAB Simulink environment. The researchers demonstrated that the efficiency of a lithium-battery-powered vehicle was comparable to that

* Corresponding authors.
E-mail addresses: j.i.ahuirtorres@ljmu.ac.uk (J.I. Ahuir-Torres), e.e.blancodavis@ljmu.ac.uk (E. Blanco-Davis).

https://doi.org/10.1016/j.seta.2026.105105
Received 4 March 2026; Received in revised form 8 May 2026; Accepted 29 May 2026
Available online 8 June 2026

of traditional and hybrid vehicles.

With respect to fuel cell modelling, a wide range of modelling approaches has been reported in the literature. In 2009, Jia et al. [12] developed the earliest model of a hydrogen fuel cell using the MATLAB Simulink platform. This model enabled simulation of the hydrogen fuel cell's dynamic response under varying load conditions. The researchers reported several key findings, including a smooth transition between system loads, the significant influence of anode and cathode pressures on hydrogen fuel cell efficiency, and the mitigation of membrane damage at low pressures. In 2015, Kabza [13] developed an accurate predictive model to assess the efficiency of the hydrogen fuel cell under varying operational conditions, including temperature, fuel flow rate, fuel concentration, reactant partial pressure, power demand, and the sizes of the anode and cathode chambers. This comprehensive study provided valuable guidance for the design and optimisation of future hydrogen fuel cells. In 2023, Vairo et al. [14] developed a model to assess the efficiency of a hybrid system comprising a hydrogen fuel cell and a diesel engine. The model was established using machine learning in combination with electrochemical impedance spectroscopy. The researchers determined that the model can predict fuel leakage as a function of hydrogen fuel cell efficiency, thereby enabling an effective method for accident prevention. In the case of the ammonia fuel cell, Ishak et al. [15] studied its performance, power-generation efficiency, and thermodynamic and electrochemical phenomena. The model was designed employing both theoretical and experimental information. They determined that the ammonia fuel cell exhibited high stability and durability at the open circuit, whereas its efficiency was higher under closed-circuit conditions due to hydrogen formation. Syed et al. [16] developed a model to assess the viability of the ammonia fuel cell as a power source and to evaluate the feasibility of solar cells and wind turbines for producing ammonia fuel. The model found that the solar cell and wind turbine were acceptable for producing ammonia fuel. The ammonia fuel cell further provided a smooth, efficient, and stable energy source.

Regarding the methanol fuel cell, Divisek et al. [17] developed a numerical model to assess its performance and efficiency. The researchers reported that the efficiency of the methanol fuel cell was significantly influenced by methanol diffusivity and fuel competition within the cell. Dohle et al. [18] further developed a theoretical model to analyse the operational mechanisms and performance of the methanol fuel cell. This model incorporated both electrochemical reactions, diffusion processes, and thermodynamic phenomena. The diffusion of methanol from the anode to the cathode resulted in a mixed potential between the two electrodes, thereby decreasing power generation efficiency. Methanol diffusion is enhanced at high concentrations in the anode chamber, thereby reducing fuel cell efficiency. Olivera et al. [19] conducted a comprehensive literature review of existing methanol fuel cell models, including numerical, simulation-based, and semi-empirical approaches. The researchers emphasised that, despite the broad range of existing methanol fuel cell models, the modelling of the two-phase flow mechanism remains a significant gap in the current literature. They also confirmed that the modelling provided a rapid and straightforward method for assessing performance degradation in methanol fuel cells.

The existing literature also encompasses the modelling of hybrid systems comprising both a battery and a fuel cell. Lemoine et al. [20] developed an algorithm to determine the optimal configuration for a hybrid energy system in maritime and aircraft transport applications, accommodating 50 passengers. The hybrid energy system comprises a battery, a hydrogen fuel cell, and a storage system. This algorithm considered both the pollution emissions, energy supplied, and the economic factors. It was developed utilising data from multiple types of lithium battery -Li-ion, Li-air, Li-S, and SBB- and fuel cells -proton exchange membrane fuel cell and solid oxide fuel cell. The researchers identified that the optimal configuration of the hybrid energy system comprising the lithium battery SSB and the solid oxide fuel cell yielded a total hydrogen consumption of 190.9 Kg of hydrogen. Although the researchers provided a valuable framework for selecting the optimal configuration of the hybrid energy system, it does not consider alternatives beyond those documented in the existing literature. Ünlübayir et al. [21] investigated the applicability of a hybrid energy system comprising a battery and a hydrogen fuel cell as energy sources for the propulsion system of a cruise ship. A representative model of the electrical and thermal behaviour of both the battery and the hydrogen fuel cell was developed for this purpose, incorporating the effect of ageing on the overall performance of the hybrid energy system. Machine learning was utilised to optimise the energy management, and the model was also validated employing hardware-in-the-loop testing. The findings demonstrated the applicability of the hybrid energy system for cruisers and proposed an optimal energy management strategy that reduced operational costs and increased energy efficiency. However, the thermodynamic and electrochemical phenomena of both the battery and the hydrogen fuel cell were ignored in the model, depending on the operating conditions. Jia et al. [22] developed a model to predict the feasibility and efficiency of using a hydrogen fuel cell to recharge a lithium battery within a hybrid system. The researchers concluded that the fuel cell can both recharge the lithium battery and supply power to electrical loads. The battery can also provide supplementary energy during periods of peak power demand. However, this model was designed explicitly for direct-current applications, which limits its broader applicability. Power demands were also simulated using a generic load resistance, thereby simplifying the load characteristics. Notably, the model was designed in MATLAB/Simulink. Motapon et al. [23] developed a predictive model to simulate a hybrid system comprising a battery or supercapacitor as the energy storage unit, a hydrogen fuel cell as the primary energy source, and an automotive vehicle as the power-demand system. In this study, the vehicle operated under alternating-current (AC) demand, necessitating a direct-current (DC)/AC converter. The researchers also assessed the most efficient energy storage system, battery or supercapacitor, to supply power to vehicles under various operational conditions, as well as the capability of the hydrogen fuel cell to recharge both energy storage systems. As a result of this investigation, they concluded that the battery exhibited higher efficiency at approximately 80% SOC and that the lowest energy consumption of the hydrogen fuel cell and the battery was achieved under frequency-decoupling and fuzzy-logic conditions. Han et al. [1] designed a model for a hybrid energy system of a low-power boat, comprising a hydrogen fuel cell and a lithium battery. The model aims to identify the optimal operation of a hybrid system by considering operational parameters such as fuel partial pressures, SOC, and dynamic power demand. They proposed an innovative hybrid system to supply the ship with energy. It is important to note that the MATLAB Simulink platform was further utilised to implement the model, and the simulation results were validated against experimental data. The researchers demonstrated that the proposed system achieved a higher relative efficiency than the traditional load command controller strategy. Bassam et al. [24] further developed a hybrid energy system model for ship applications, using multiple energy management strategies to identify optimal conditions with respect to energy and fuel consumption. In this study, the specifications of the *FCS Alterwasser* were adopted to model the ship. The multi-scheme energy management strategy included state-based, equivalent-fuel-consumption minimisation, charge-depleting and charge-sustaining, and a classical proportional-integration controller-based approach. The models were designed in MATLAB Simulink. The results indicated that both state-based and proportional integration effectively reduce fuel consumption, whereas battery SOC significantly influences overall energy consumption. Switching between operational schemes incurs only a negligible additional energy or fuel consumption. Nui and Xiao [25] conducted a comparative study of the efficiencies of the energy management strategy and topology optimisation method for a cruise ship propellowered by a hybrid energy system comprising a battery and a hydrogen fuel cell stack. The model was developed in the MATLAB Simulink environment, and the simulations represented various operational scenarios of the cruise ship, including cruising, docking, and sailing. The topological optimisation method demonstrated superior efficiency in energy distribution for the energy management system, reducing power fluctuations in the hydrogen fuel cell and the battery. Notably, both the hydrogen fuel cell and the battery supplied power directly to the system simultaneously. Nazemian et al. [26] also investigated the implementation of various energy management strategies in a hybrid energy system model comprising a lithium battery and a hydrogen fuel cell, which supplied power to the propellers of the crew transfer vessels. Energy management strategies employed in the simulations included state-based, equivalent-fuel-consumption minimisation, charge-depleting and charge-sustaining strategies, multi-scheme strategies, and a classic proportional-integral-controlled base. The models were designed utilising the MATLAB Simulink environment. The multi-schemes exhibited the highest energy efficiency among the energy management strategies examined. It is important to note that the electrochemical and thermodynamic equations were absent in this study. Jamma et al. [27] conducted a comparable investigation into the applicability of a hybrid energy system comprising a lithium battery and a hydrogen fuel cell for maritime transport, employing modelling in MATLAB Simulink. In this case, the researchers proposed an innovative energy management strategy that demonstrated excellent efficiency in temporal energy distribution.

Although fuel cells, batteries, and hybrid energy systems have been extensively modelled across a wide range of applications and operating conditions, evaluating fuel cell efficiency for battery recharging by fuel cell type remains a notable gap in the existing literature. This paper presents a theoretical investigation of fuel cell efficiency for battery recharging as a function of fuel type, including hydrogen, ammonia, and methanol. Seven scenarios were proposed in this study, encompassing configurations comprising single-type fuel cells (hydrogen, ammonia, and methanol) and multiple-type fuel cells (hydrogen/ammonia, hydrogen/methanol, ammonia/methanol, and hydrogen/ammonia/methanol). Both battery and fuel cell blocks of the model were developed using the governing thermodynamic and electrochemical equations. The model was developed based on lithium battery specifications and implemented in MATLAB Simulink. The recharging and discharging processes were defined over the SOC range from 0% to 100%. The efficiency of lithium battery recharging was defined as inversely proportional to recharging time. The total simulation duration was set to 4 days to ensure statistical significance in recharging time measurements.

Simulation methodology

The system model for charging a lithium battery using a fuel cell (Fig. 1) was developed utilising the MATLAB Simulink environment. Separate models were developed for three distinct types of fuel cells, differentiated by their respective fuel sources: hydrogen, ammonia, and methanol. Although the specific fuel cell model varied with the fuel type, several blocks were similar. The fuel cell block simulated the generation of electrical energy using the selected fuel. "Direct current (DC) / DC converter" block was employed to model the conversion of the fuel cell output to a DC voltage compatible with the battery system. "Discharging/charging controller" block regulated the discharge/recharging cycles of the batteries. The power supply from the fuel cell to the lithium battery was automatically terminated when the battery state-of-charge (SOC) reached the predefined fully charged threshold (recharged SOC) and reactivated when SOC decreased to the specific threshold (discharged SOC), both detailed in Section "Simulation setup". The "Lithium battery" block simulated lithium battery behaviour according to its commercial specifications. The "DC / AC converter" block modelled the conversion of the battery's DC outputs into the AC requirements of the connected electrical load. The fuel cell was electrically connected to the battery via the "DC / DC converter" and "Discharging/charging controller" blocks.

In contrast, the "DC / AC converter" block connected the battery to the AC power load. This power demand was modelled using the "Load" block, which comprises a 1 Ω resistor connected to the "DC / AC converter" block and ground. Notably, the battery served solely as a power supply to the AC load.

Fuel cell models

The modelling of the fuel cell was based on the Nernst equations for the electrochemical processes (Eq. (1) [16,22,23,28,29]).

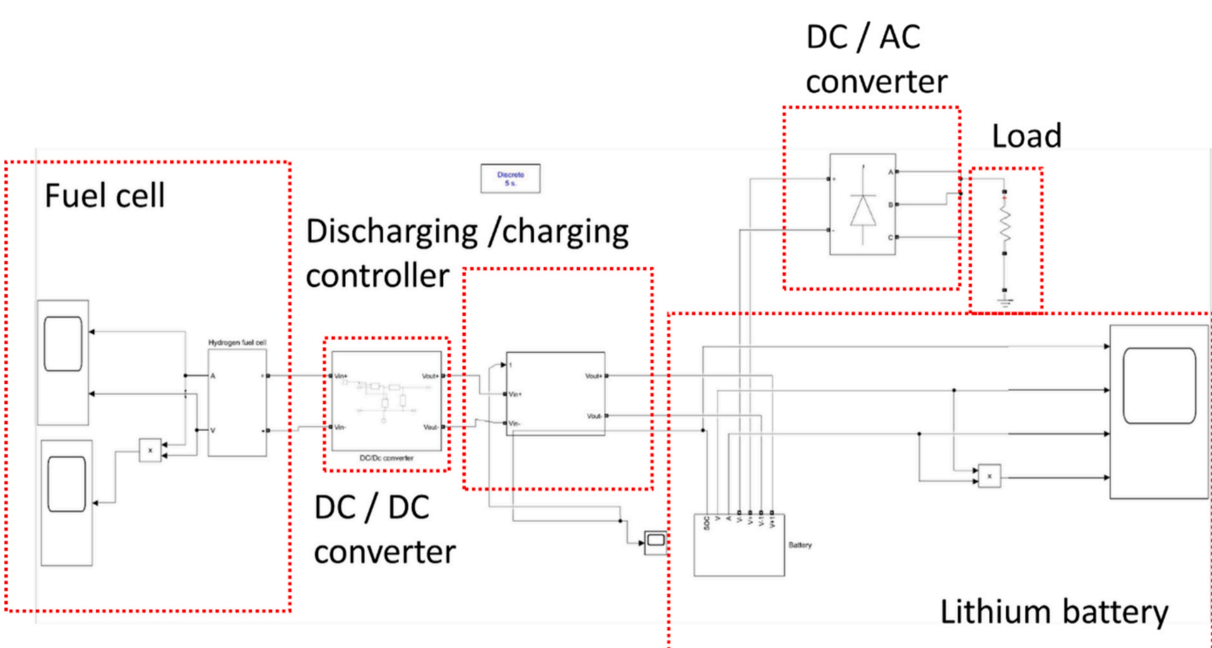

Fig. 1. Schematic drawing of the discharging/recharging model of the lithium battery using a fuel cell, comprising the following functional blocks: "fuel cell", "DC / DC converter", "Discharging/charging controller", Lithium battery", DC / AC converter", and "Load".

$$E = N[E_{ocp} + RTF^{-1}n_e^{-1}[(\ln([Rea]^m[Pro]^{-n}) - \ln(ii_o^{-1}) + \alpha^{-1}\ln(1 - ii_l^{-1})] - R_{ohm}i] \tag{1}$$

where, E is the voltage of the fuel cell in operation mode, N is the number of the fuel cells in the stacks, E_{ocp} is the voltage of the fuel cell for open circuit, R is the ideal gas constant (8.314 $JK^{-1}mol^{-1}$), T is the temperature, F is the Faraday's constant (96500 $Cmol^{-1}$), n_e is the electrons transferred in the electrochemical reactions, $[Rea]^m$ is the partial pressure with the stoichiometric power factor of the reactants, $[Pro]^{-n}$ is the partial pressure with the stoichiometric power factor of the products, R_{ohm} is the ohm resistance, i is the current produced by the fuel cell, i_o is the current of the fuel cell in the open circuit, α is the cathodic slope, and i_l is the current limit of the fuel cell. It is noteworthy that only gaseous state chemical agents participated in the electrochemical reaction within the fuel cell.

The model used to simulate fuel cell power generation is presented in Fig. 2. In this model, the relative pressures of the reactants and products were assumed to vary over time. It was represented through the simulation block named "Fuel pressure in the anode and cathode". The flow within the anode and cathode (F_{cham}) chamber was described by Eq. (2) [22,23].

$$F_{cham} = P_{in} - mRTiF^{-1}n_e^{-1}V^{-1} + nRTiF^{-1}n_e^{-1}V^{-1} \tag{2}$$

Here, P_{in} is the pressure in the chamber, m is the stoichiometric power factor of the reactants, n is the stoichiometric factor of the product, and V is the volume of the chamber.

The fuel cell characteristics were implemented as a simulation block to represent the intrinsic features of the cells, including temperature, the number of cells per stack, and the dimensions of the cathode and anodic chambers. E_{ocp} was defined using Eq. (3) [13,15,28,29], implemented in the model via the "Voltage at open circuit potential" block.

$$E_{ocp} = F^{-1}n_e^{-1}(\Delta H - T\Delta S) \tag{3}$$

where, ΔH and ΔS are the enthalpy and entropy of the electrochemical reactions, respectively. The block entitled "Combustion products" represented the products of the electrochemical reactions. The "Internal resistance of the fuel cell" block implemented part of Eq. (1) $-R_{ohm}i - \ln(ii_o^{-1}) + \alpha^{-1}\ln(1 - ii_l^{-1})$ in the model. R_{ohm} was determined by Eq. (4) [1–3].

$$R_{ohm} = TRNn_e^{-1}F^{-1}\alpha^{-1}(i_{nom} - 1)^{-1}\ln(i_o) \tag{4}$$

Here, i_{nom} is the nominal current, which was estimated by Eq. (5) [2,4,5].

$$i_o = K_B R^{-1}F^{-1}N_a^{-1}\left(\sum P_{Rea}\right)e^{-\Delta G/RT} \tag{5}$$

Here, K_B is Boltzmann's constant, N_a is Avogadro's number, P_{Rea} is the partial pressure of the reactants, and ΔG is the Gibbs energy differential. The products of the electrochemical reactions varied with temperature. It is important to note that water is included in the equation only when the fuel cell temperature is at or above 373 K. The liquid chemical products were absent in the electrochemical reactions, which were represented using the "Temperature effect on the fuel cell" block. The current generated by the fuel cell was constrained by its operating conditions (e.g., fuel partial pressures, temperature, fuel type, humidity, number of cells, and anodic and cathodic chamber dimensions), which were implemented in the model through the "Current controller" block. Finally, the model block titled "External connector" served as the interface between the fuel cell and the central system.

Cell features for the fuels hydrogen, ammonia, and methanol are listed in Table 1.

Lithium battery

The model for the lithium battery was also developed based on the electrochemical mechanism, as represented by Eq. (6) [22,23,27,31].

$$E_{Bat} = E_{nom} - AQ\left(Q - \int i_{Bat} + \int i_{char}\right)^{-1} + Be^{-C\int i_{Bat} - \int i_{char}} - R_{pol} \tag{6}$$

where, E_{Bat} is the supplied voltage, E_{nom} is the nominal voltage, A is the polarisation voltage, Q is the maximum capacity, i_{Bat} is the positive current, i_{char} is the charged current from the fuel cell, B is the exponential voltage, C is the exponential capacity, and R_{pol} is the polarisation resistance, calculated using Eq. (7) [1,3,6].

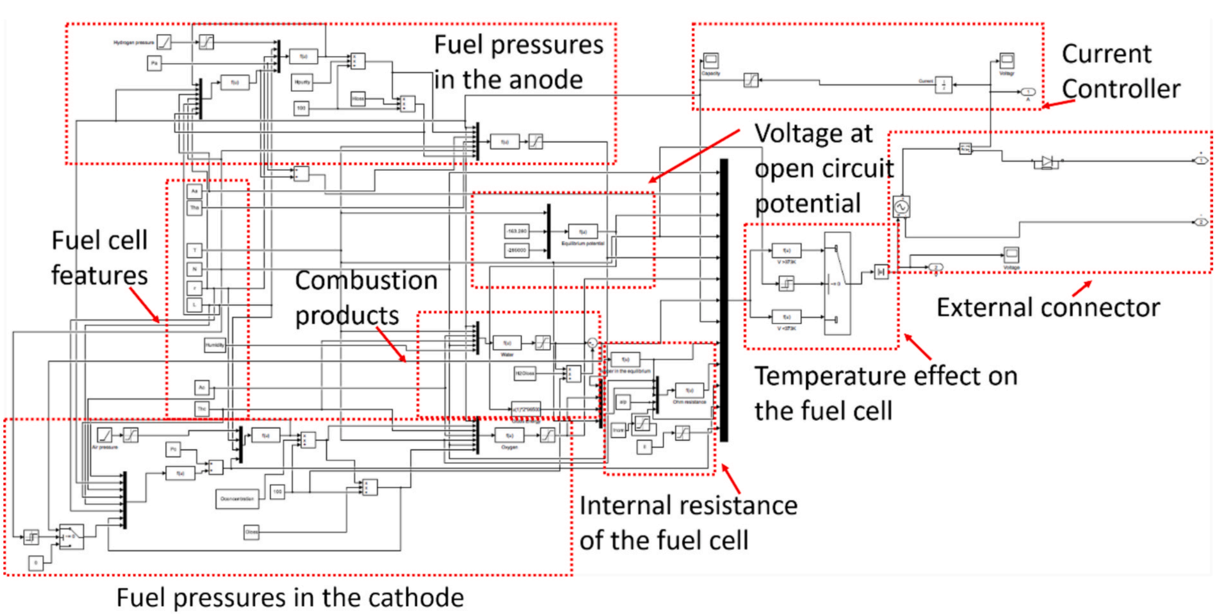

Fig. 2. Schematic drawing of the fuel cell model, formed of the following functional blocks; "Fuel pressures in the cathode", "Fuel cell features", "Combustion products", "Fuel pressures in the anode", "Voltage at the open circuit potential", "Internal resistance of the cell", "Temperature effect on the fuel cell", "Current controller", and "External connector".

Table 1
Fuel cell conditions by fuel type.

Parameter	Fuel type		
	Hydrogen [1,13,22]	Ammonia [15,29]	Methanol [17,18,30]
Anode reaction	$2H_2 \rightarrow 4H^+ + 4e^-$	$4NH_3 \rightarrow 12H^+ + 2N_2 + 12e^-$	$2CH_3OH + 2H_2O \rightarrow 2CO_2 + 12H^+ + 12e^-$
Cathode reaction	$O_2 + 4e^- \rightarrow 2O^{-2}$	$3O_2 + 12e^- \rightarrow 6O^{-2}$	$3O_2 + 12e^- \rightarrow 6O^{-2}$
Products	$2H_2O$	$6H_2O, and 2N_2$	$4H_2O, and 4CO_2$
n_e	4	12	12
$\Delta H(\text{kJmol}^{-1})$	−285.93	46	−700
$\Delta S(\text{JK}^{-1}\text{mol}^{-1})$	−163.42	98.9	−242.6
Purity	21	21	21
$i_l(\text{Acm}^{-2})$	320	94	40
$i_{nom}(\text{Acm}^{-2})$	250	50	20
Maximum voltage (V)	0.70	1.24	0.9

$$R_{pol} = i_{Bat}AQ[(1 - i_{neg})\left(Q - \int i_{Bat} + \int i_{char}\right)^{-1} - i_{neg}\left(\int i_{Bat} + \int i_{char} - 0.1Q\right)^{-1} \quad (7)$$

Here, i_{neg} is the negative value of the current. Several blocks were incorporated into the lithium battery model to accurately represent its electrochemical behaviour (Fig. 3). The instantaneous battery capacity was modelled using the "Capacity monitoring" block. At the same time, the state of charge (SOC) was represented through the "SOC monitoring" block. SOC evolution was calculated using Eq. (8) [10,23,32].

$$SOC = 100\left(1 - \left(\int i_{Bat} + \int i_{char}\right)Q^{-1}\right) \quad (8)$$

The battery's operating periods were defined either by SOC thresholds or by time intervals via the switch-on/off controller. The "Voltage converter" block generated the battery voltage as a function of time according to Eq. (6). The battery's instantaneous current was modelled using the "Direct battery current generator" block, implemented as a first-order filter. The "Voltage function generator" block was utilised to realise Eq. (6), whereas the "Current converter" block transformed the generated voltage signal into its corresponding current. The "Delay" block was introduced to break the feedback loop arising from the dependence of Eq. (6) on the current. The negative current associated with battery discharge was modelled using the "Negative current generator" block. The battery's expended capacity was estimated by integrating the current over time using the "Capacity generator" block. The "Battery internal resistance" block modelled the battery's internal resistance, which was in parallel with the "Voltage function generator" block. The "Electrical connector to power required" block was used to link the battery to an external load. In contrast, the "Electrical connector to power source" block was employed to connect the battery to the fuel cells.

Simulation setup

Simulations aimed at evaluating battery recharging efficiency as a function of the fuel cell type. To achieve this aim, seven scenarios were considered according to the cell fuel type, including hydrogen (H), ammonia (A), methanol (M), hydrogen and ammonia (H&A), hydrogen and methanol (H&M), ammonia and methanol (A&M), and hydrogen, ammonia and methanol (H&A&M). The dimensions of the anodic and cathodic chambers remained constant across all scenarios. The total area of both chambers was 100 cm^2, while the chamber thicknesses were 0.12 cm and 0.65 cm for the anodic and cathodic chambers, respectively. The humidity in all simulation scenarios was kept at 80%. The operating temperature was identical across all scenarios and was maintained at 298K. Simulation conditions were further adjusted to ensure comparable conditions across all scenarios, as summarised in Table 2.

The conditions of the Motorola 12.8V lithium battery were used to model the battery in the simulation. The corresponding specifications are summarised in Table 3.

Notably, the total simulation duration was set to 4 days (3.6×10^5 s), and the charging process started at 0 % SOC and terminated upon reaching 100 % SOC.

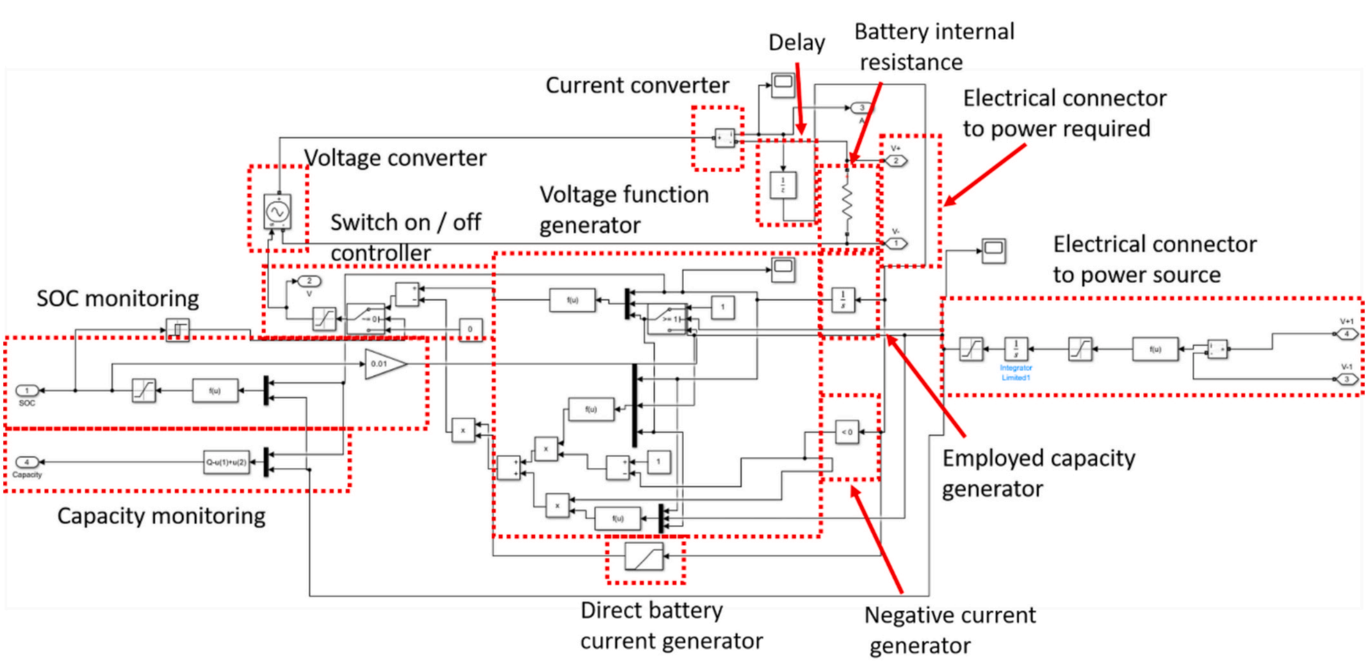

Fig. 3. Schematic drawing of the lithium battery model, consisting of the following blocks; "Capacity monitoring", "SOC monitoring", "Voltage converter", "Switch on / off controller", "Voltage function generator", "Direct battery current generator", Current converter", "Delay", "Battery internal resistance", "Negative current generator", "Electrical connector to power required", "Employed capacity generator", and "Electrical connector to power source".

Table 2
Simulation conditions of the fuel cell.

Scenario	Cell types	Total air pressure for the cell system (at)	Total fuel pressure for the cell system (at)	Cell number
H	Hydrogen	13.92	13.92	60
A	Ammonia	13.92	13.92	60
M	Methanol	13.92	13.92	60
H&A	Hydrogen	6.86	6.86	30
	Ammonia	6.86	6.86	30
H&M	Hydrogen	6.86	6.86	30
	Methanol	6.86	6.86	30
A&M	Ammonia	6.86	6.86	30
	Methanol	6.86	6.86	30
H&A&M	Hydrogen	3.43	3.43	20
	Ammonia	3.43	3.43	20
	Methanol	3.43	3.43	20

Table 3
Lithium battery specification: 12.8 V.

Parameter	Value
Q(Ah)	100
E_{ocp}(V)	12.8
Battery internal resistance (Ω)	0.15
Potential limit (V)	15
Current limit (A)	100
A(Ah)	0.128
B(Vs^{-1})	22
C(Vh)	17.186

Results

The temporal evolution of the lithium battery features (voltage, current, power, and SOC) were different for the charging and discharging stages (Fig. 4). However, the voltage (Fig. 4(a)), current (Fig. 4(b)), and power (Fig. 4(c)) of the battery obviously exhibited similar temporal trend for both the charging and discharging stages. The behaviour of the charging stage differed from the discharging stage. During the recharging stage, the battery features remained at 0 because the device was inactive. During the discharge process, the battery characteristics exhibited several stages of temporal evolution. In the initial period (3200 s), the features decreased exponentially with time, corresponding to the exponential response region of the battery discharge stage. This rapid decline is attributed to the battery's initially high capacity, which is quickly depleted [23]. Following this reduction, the battery's voltage, current, and power remained constant for an extended period, indicating the battery was operating within its normal operating region [22]. At the last stage (26000 s), the battery current, voltage, and power rapidly decreased to zero within milliseconds, indicating complete discharge [22,23].

In contrast, SOC behaviour during both the charging and discharging stages differed from that of the previously noted features. During the charging stage, SOC increased linearly with time, whereas during the discharging stage, SOC decreased linearly. These trends are consistent with the realistic trends of lithium-ion batteries reported in the existing literature [10,31,33]. It is important to note that the magnitudes of the battery features, including voltage, current, and power, reported in the existing experimental literature differed from those of the study, due to the use of distinct lithium battery models across the referenced works.

It is important to note that the temporal localisation of the recharging and discharging stages shifted, with the magnitude of the displacement determined by the configuration. These observations highlight the pronounced influence of the fuel cell type and configuration on the recharging/discharging behaviour, which is discussed in the subsequent sections.

The temporal evolution of the fuel cell voltage, current, and power varied across different scenarios (Fig. 5).

The current (Fig. 5(a)) and power (Fig. 5(b)) exhibited comparable temporal behaviour, characterised by two stages corresponding to the battery's discharging and recharging. This observation indicates strong coupling between battery processes and fuel cell power generation, with current playing a predominant role in determining power output. During battery discharge, both current and power remained zero. This observation can be attributed to their electrochemical reactions at near-equilibrium conditions (open circuit) [15]. In contrast, during battery recharging, both current and power increased sharply within the first milliseconds and then remained constant. This finding indicates a steady recharging regime driven by the fuel cells. At the final stage of the recharging process, both fuel cells exhibit a dramatic drop to zero, marking the end of charging and the beginning of the discharge stage. The values and time evolution of current and power depended on the specific scenario considered. However, the areas under the time–current and time-power curves were comparable across all scenarios. Scenarios characterised by elevated power or current values exhibited shorter processing times, whereas the opposite was observed. These findings validated the accuracy of the recharging process simulation, as all fuel cell system configurations must supply an equivalent amount of energy or charge to satisfy the battery's demands [6]. The power and current levels across the scenarios followed the order: M > H > A&M > H&M > H&A > A > H&A&M. This hierarchy is discussed in detail in the subsequent section. It is noteworthy that temporal trends of the fuel cell features - voltage, current, and power - were comparable to those reported for hydrogen [32,33], ammonia [29], and methanol [34,35] fuel cells in the existing literature. However, temporal trends for scenarios incorporating multiple types of fuel cells were absent from the existing literature, owing to the novelty of the scenarios investigated in the present study.

With respect to the voltage (Fig. 5(b)), most scenarios exhibited temporal evolutions comparable to those observed for power and current. In contrast, Scenario A, which comprised only ammonia fuel cells, showed a reduction in voltage during recharging. This behaviour is attributed to the endothermic nature associated with their electrochemical reactions [15]. This phenomenon was absent in the other scenarios that combined the ammonia fuel cell with other fuel cell types, because the additional fuel cells compensated for the voltage deficiency. This limitation can be mitigated by implementing an auxiliary heating source to facilitate electrochemical reactions in the ammonia fuel cell. All fuel cell systems exhibited a constant voltage during discharge, consistent with the fuel cell's open-circuit potential.

The recharging time for the investigated scenarios exhibited an order opposite to that observed for the current: M < H < A&M < H&M < H&A < A < H&A&M (Fig. 6). It is important to note that the recharging efficiency is considered inversely proportional to the time of recharging. The highest recharging efficiency was observed in scenario M, which is attributed to the relatively high exothermicity of the electrochemical reactions in the methanol fuel cell [17]. However, the combustion of methanol produces carbon dioxide, a greenhouse gas [17,18], which is a significant drawback of this technology for marine transport applications. H scenario exhibited the second-shortest recharging process, owing to the exothermic nature of hydrogen combustion [4,28,36]. The third-highest recharging efficiency was observed in the A&M scenario because the relatively high recharging efficiency of the methanol fuel cell partially offset the low recharging efficiency of the ammonia fuel cell. A discrepancy arises because the H&M scenario exhibited a lower recharging efficiency than the A&M scenario. In principle, the H&M configuration should exhibit higher recharging efficiency than the A&M

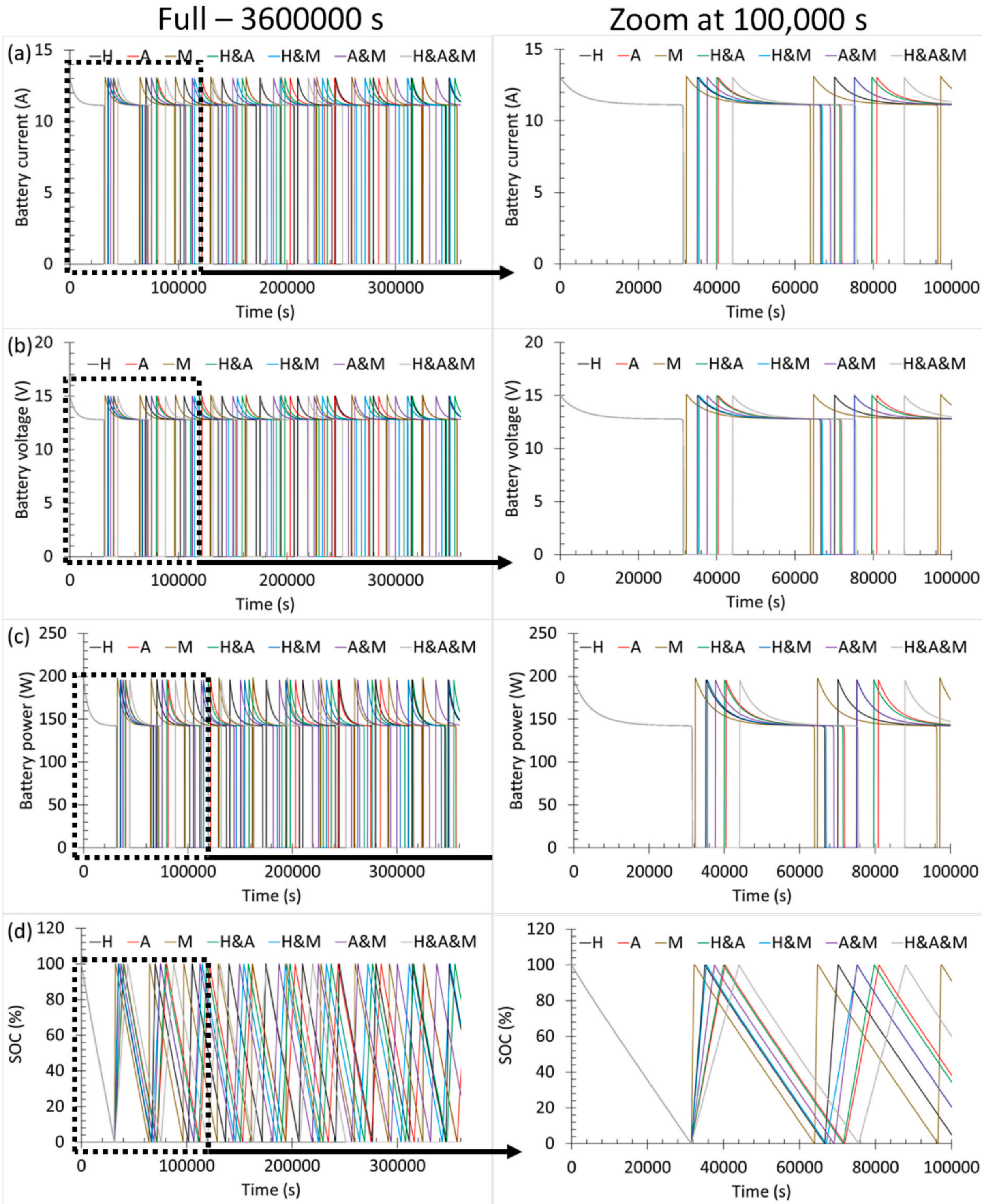

Fig. 4. Temporal evolution of the lithium battery current (a), voltage (b), power (c), and SOC (d) during charging and discharging cycles for the different scenarios. Left graphs depict the full temporal evolution (360,000 s) of lithium battery characteristics, and the right graphs are magnifications at a time scale of 100,000 s of the left graphs.

scenario, owing to the higher individual efficiencies of the two fuel cells. However, in this scenario, the different types of fuel cells affect their fuel consumption, reducing the overall recharging efficiency. A reduction in fuel consumption within the fuel cell decreases both the flow rates into the anodic and cathodic chambers and the efficiency of their electrochemical reactions, thereby reducing the fuel cell's power generation. The recharging efficiency ranking of configuration H&A is attributed to the hydrogen fuel cell's limited capacity to compensate for the low efficiency of the ammonia fuel cell. It is noteworthy that the power contribution of the hydrogen fuel cell was lower than that observed in the methanol fuel cell. The lowest recharging efficiency observed in the ammonia fuel cell can be attributed to the endothermic nature of

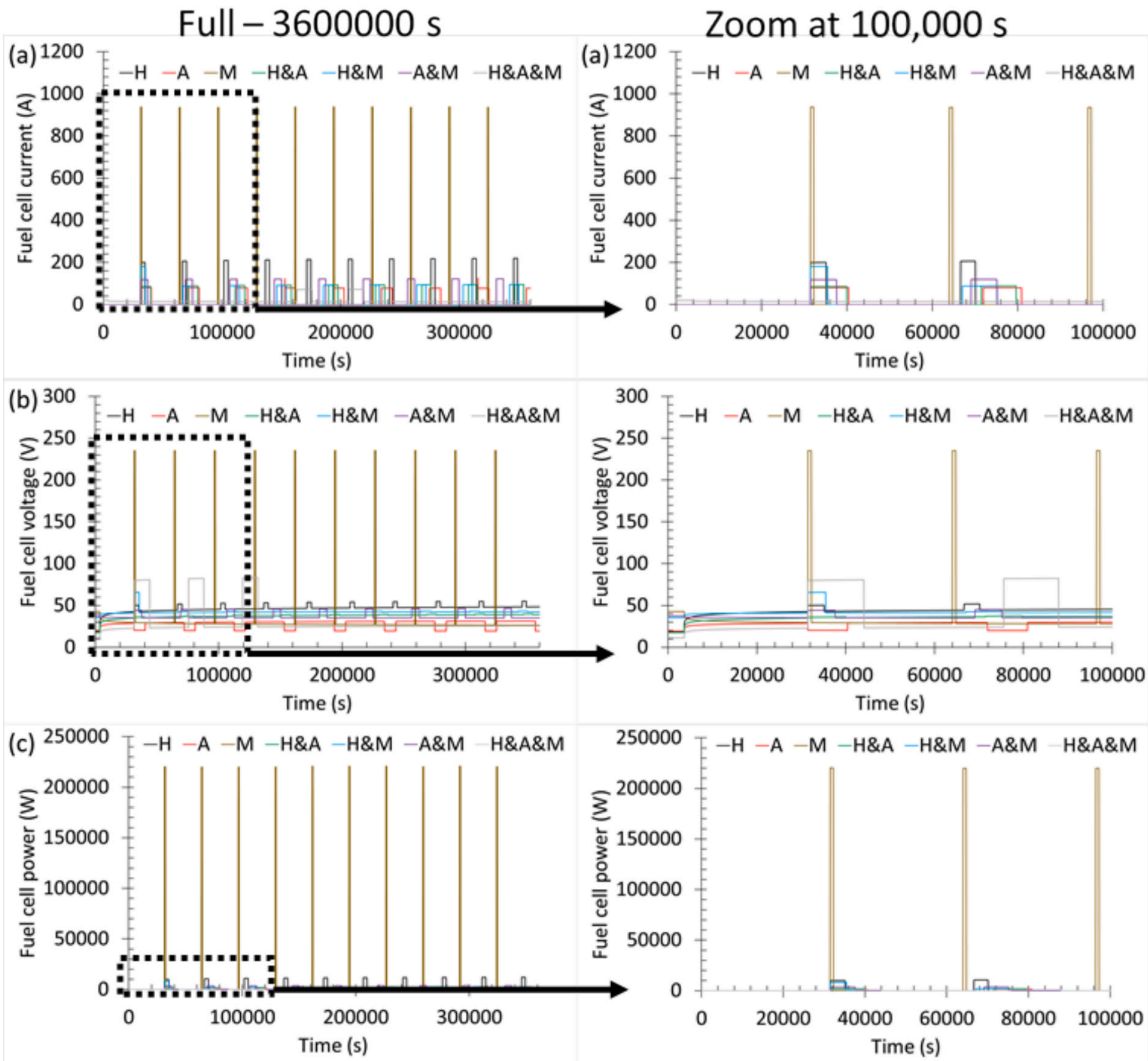

Fig. 5. Temporal evolution of the fuel cell current (a), voltage (b), and power (c) during charging and discharging cycle processes according to the different scenarios. The left graphs depict the total temporal evolution of lithium battery characteristics, and the right graphs are magnifications of the left graphs at 100,000 s.

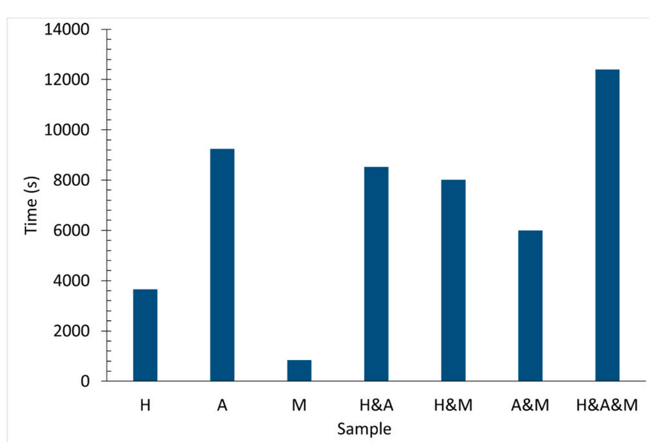

Fig. 6. Full recharging time of the lithium battery according to the scenario configuration.

ammonia combustion reactions [15]. Finally, the scenario exhibited H&A&M the lowest recharging efficiency, which is associated with both the competitive interaction between hydrogen and methanol fuel cells and the relatively low efficiency of the ammonia fuel cell.

The theoretical results of this study establish a clear hierarchy in recharging efficiency, with methanol and hydrogen configurations outperforming those involving ammonia or multi-fuel combinations. Methanol's high efficiency is largely attributed to the significantly exothermic nature of its electrochemical reactions [17,18]. Hydrogen follows closely, also benefiting from exothermic combustion [4]. Conversely, ammonia exhibits the lowest efficiency among single-fuel scenarios due to the endothermic nature of its combustion, which reduces voltage during the recharging process [15]. While these findings provide a vital baseline for selecting power sources, the practical deployment of these technologies in the maritime sector involves significant trade-offs regarding safety, storage, and environmental impact that go beyond simple recharging time [37,38].

One of the most critical practical constraints is the disparity in fuel storage and handling requirements. While methanol is the most efficient according to the model, its primary drawback is the production of carbon dioxide, which challenges the IMO's net-zero 2050 goals unless carbon-neutral "green" methanol is utilised [39,40]. On the other hand, its storage is relatively easy using near-conventional tanks and systems, enabling retrofits and relatively low disruption [41]. Hydrogen, while a zero-emission fuel, poses immense logistical challenges due to its low density, which necessitates high-pressure or cryogenic storage tanks that occupy substantial volume and add weight to a vessel [42,43]. Ammonia offers a middle ground as a carbon-free carrier, as it is easier to liquefy than hydrogen. Still, its high toxicity and corrosive properties necessitate specialised materials and rigorous safety protocols to protect the crew and the marine environment [44,45].

System weight and volume also play a pivotal role in maritime design, where cargo space is at a premium [46]. The study notes that configurations using multiple fuel cell types, such as the three-type hydrogen, ammonia, and methanol system, resulted in the lowest recharging efficiency due to competitive fuel consumption and unfavourable interactions. Beyond this loss of efficiency, such multi-fuel systems would drastically increase the physical footprint and mechanical complexity of the ship's engine room [41,45,47]. This suggests that while multi-fuel systems might seem versatile, the added weight and the efficiency penalties observed in the simulation make them less viable than optimised single-fuel systems [47].

Economic factors and the realities of dynamic operating conditions further complicate the transition to hybrid fuel-cell-battery systems. The current simulation assumes a steady-state recharging regime under constant conditions. However, real-world marine power demands are highly variable, requiring systems that can handle rapid load fluctuations without significant degradation [6,48,49]. Furthermore, the total cost of ownership, including the price of "green" fuels and the lack of global bunkering infrastructure for hydrogen and ammonia, remains a barrier [45,50]. Therefore, while this research identifies methanol and hydrogen as more efficient options for battery recharging, the final selection for maritime applications must balance these theoretical efficiencies against the practical realities of safety, storage volume, and economic feasibility [41,43].

The integration of a battery energy storage system serves as a critical technical buffer, bridging the gap between the steady-state simulations presented in this study and the highly dynamic reality of marine power demand [49,51]. While the current model assumes constant recharging conditions, real-world maritime operations involve rapid load fluctuations due to manoeuvring and sea states that can cause significant degradation of fuel cell membranes if these transients are forced to be followed directly [52]. By utilising the battery as a "peak-shaver," the fuel cell can maintain a stable, near-constant output at its optimal efficiency point, specifically leveraging the exothermic advantages of methanol and hydrogen identified in the research. In contrast, the battery handles peak demand and instantaneous power surges [53,54]. This hybrid configuration not only protects the system from the mechanical and chemical stresses of variable operation but also allows for a smaller, more efficient fuel cell stack that operates continuously to maintain the battery's state of charge, thereby enhancing the overall reliability and lifespan of the vessel's power plant [49].

Conclusions

This study presents a theoretical investigation into the efficiency of various fuel cell configurations for recharging a lithium battery. These configurations encompassed several scenarios involving systems with distinct fuel cell types, including hydrogen, ammonia, and methanol fuel cells, as well as single- and multi-fuel-cell systems. The key findings of this study are presented below.

1. The temporal evolution of the discharging and recharging processes in the lithium battery can be simulated using the study model, which captures the behaviour of voltage, current, power, and SOC during these processes.
2. The temporal behaviour of the fuel cell features - voltage, current, and power - for distinct fuels, including hydrogen, ammonia, and methanol, and under varying operational conditions of the battery (recharging and discharging) can be represented using the model of the study.
3. Fuel cell features exhibit distinct trends depending on both the battery operating mode and the type of fuel used. During the discharging process, the current and power remain zero, whereas the voltage remains constant. During the recharging process, both current and power increase sharply across all fuel cells; however, their magnitudes and durations vary with the fuel cell type. For most fuel cells, the voltage follows a temporal evolution similar to that observed for current and power. A notable deviation is observed in the ammonia fuel cell, where the voltage is markedly reduced during recharging.
4. The recharging efficiency of the fuel cells is defined as the inverse of the recharging time and is therefore scenario-dependent. The methanol fuel cell scenario exhibits the highest recharging efficiency, followed by the hydrogen fuel cell configuration. Overall, scenarios that combine battery types have generally demonstrated lower recharging efficiency than scenarios based on a single battery type. An exception is observed for the ammonia fuel cell, which exhibits the second-lowest recharging efficiency among the scenarios configured with a single fuel cell type. The lowest recharging efficiency is observed for the scenario with the configuration comprising three different types of fuel cells.

This study provides essential findings on the optimal selection of a fuel cell for lithium-ion battery recharging, representing a significant advancement for the marine transport industry. Beyond marine transport applications, these findings are also applicable to other industrial sectors, including automotive, construction, and aerospace.

Author Contributions

All authors contributed to the study conception and design. J.I.A.T. developed the models and assessed and discussed the simulation data. The first draft of the manuscript was written by all authors (J.I.A.T., O. Y., E.E.B.D., V.S., D.H., and J.W.), commented on, and subsequently revised. All authors have read and approved the final manuscript.

CRediT authorship contribution statement

J.I. Ahuir-Torres: Writing – review & editing, Writing – original draft, Methodology, Investigation, Formal analysis, Data curation, Conceptualization. **O. Yuksel:** Writing – review & editing. **E. Blanco-**

Davis: Writing – review & editing. **G.V. Shagar:** Writing – review & editing. **D. Hitchmough:** Writing – review & editing. **J. Wang:** Writing – review & editing.

Declaration of competing interest

The authors declare that they have no known competing financial interests or personal relationships that could have appeared to influence the work reported in this paper.

Acknowledgements

This research was funded by Retrofit Solutions to Achieve 55% GHG Reduction by 2030, grant number 10064483 from UKRI and from the EU (grant number: Horizon Europe 101096068).

Data availability

Data will be made available on request.

References

[1] Han J, Charpentier J-F, Tang T. An energy management system of a fuel cell/battery hybrid boat. Energies 2014;7:2799–820. https://doi.org/10.3390/en7052799.
[2] Yuksel O. A comprehensive feasibility analysis of dual-fuel engines and solid oxide fuel cells on a tanker ship considering environmental, economic, and regulation aspects. Sustainable Prod Consum 2023;42:106–24. https://doi.org/10.1016/j.spc.2023.09.012.
[3] Mahdi H, Hoff B, Østrem T. A review of power converters for ships electrification. IEEE Trans Power Electron 2023;38:4680–97. https://doi.org/10.1109/TPEL.2022.3227398.
[4] Perčić M, Vladimir N, Koričan M. Electrification of inland waterway ships considering power system lifetime emissions and costs. Energies 2021;14:7046. https://doi.org/10.3390/en14217046.
[5] Lucà Trombetta G, Leonardi SG, Aloisio D, Andaloro L, Sergi F. Lithium-ion batteries on board: a review on their integration for enabling the energy transition in shipping industry. Energies 2024;17. https://doi.org/10.3390/en17051019.
[6] Xie P, Asgharian H, Guerrero JM, Vasquez JC, Araya SS, Liso V. A two-layer energy management system for a hybrid electrical passenger ship with multi-PEM fuel cell stack. Int J Hydrogen Energy 2024;50:1005–19. https://doi.org/10.1016/j.ijhydene.2023.09.297.
[7] Inal OB, Zincir B, Dere C, Charpentier J-F. Hydrogen Fuel Cell as an Electric Generator: A Case Study for a General Cargo Ship. Journal of Marine Science and Engineering 2024, Vol 12, Page 432 2024;12:432–432. doi:10.3390/JMSE12030432.
[8] Saxena S, Hendricks C, Pecht M. Cycle life testing and modeling of graphite/LiCoO2 cells under different state of charge ranges. J Power Sources 2016;327:394–400. https://doi.org/10.1016/j.jpowsour.2016.07.057.
[9] Sepasi S, Ghorbani R, Liaw BY. Inline state of health estimation of lithium-ion batteries using state of charge calculation. J Power Sources 2015;299:246–54. https://doi.org/10.1016/j.jpowsour.2015.08.091.
[10] Kumar RR, Bharatiraja C, Udhayakumar K, Devakirubakaran S, Sekar KS, Mihet-Popa L. Advances in batteries, battery modeling, battery management system, battery thermal management, SOC, SOH, and charge/discharge characteristics in EV applications. IEEE Access 2023;11:105761–809. https://doi.org/10.1109/ACCESS.2023.3318121.
[11] Chatterjee P, Singh J, Singh R, Avadh YAR, Kanchan S. Electric vehicle modeling in MATLAB and simulink with SoC &SoE estimation of a lithium-ion battery. IOP Conf Ser: Mater Sci Eng 2021;1116:012103. https://doi.org/10.1088/1757-899X/1116/1/012103.
[12] Jia J, Yang S, Wang Y, Cham YT. Matlab/Simulink based-study on PEM fuel cell and nonlinear control. IEEE Int Conf Control Autom 2009;2009:1657–62. https://doi.org/10.1109/ICCA.2009.5410529.
[13] Kabza A. Fuel cell formulary. Kabza, Ed 2015. https://kabza.de/pemfc.de/FCF_Smart.pdf (accessed April 20, 2026).
[14] Vairo T, Cademartori D, Clematis D, Carpanese MP, Fabiano B. Solid oxide fuel cells for shipping: a machine learning model for early detection of hazardous system deviations. Process Saf Environ Prot 2023;172:184–94. https://doi.org/10.1016/j.psep.2023.02.022.
[15] Ishak F, Dincer I, Zamfirescu C. Thermodynamic analysis of ammonia-fed solid oxide fuel cells. J Power Sources 2012;202:157–65. https://doi.org/10.1016/j.jpowsour.2011.10.142.
[16] Syed MA, Siddiqui O, Kazerani M, Khalid M. Analysis and modeling of direct ammonia fuel cells for solar and wind power leveling in smart grid applications. IEEE Access 2024;12:46512–23. https://doi.org/10.1109/ACCESS.2024.3376513.
[17] Divisek J, Fuhrmann J, Gärtner K, Jung R. Performance modeling of a direct methanol fuel cell. J Electrochem Soc 2003;150:A811. https://doi.org/10.1149/1.1572150.
[18] Dohle H, Divisek J, Jung R. Process engineering of the direct methanol fuel cell. J Power Sources 2000;86:469–77. https://doi.org/10.1016/S0378-7753(99)00456-5.
[19] Oliveira VB, Falcão DS, Rangel CM, Pinto AMFR. A comparative study of approaches to direct methanol fuel cells modelling. Int J Hydrogen Energy 2007;32:415–24. https://doi.org/10.1016/j.ijhydene.2006.06.049.
[20] Lemoine B, Caliandro P, Wannemacher T, Baumann N, Vezzini A. Energy Storage System Hybridization Algorithm for Mobility Applications Based on Future Battery and Fuel Cell Technologies. 2023 IEEE International Conference on Electrical Systems for Aircraft, Railway, Ship Propulsion and Road Vehicles & International Transportation Electrification Conference (ESARS-ITEC), 2023, p. 1–6. doi:10.1109/ESARS-ITEC57127.2023.10114853.
[21] Ünlübayir C, Youssfi H, Khan RA, Ventura SS, Fortunati D, Rinner J, et al. Comparative analysis and test bench validation of energy management methods for a hybrid marine propulsion system powered by batteries and solid oxide fuel cells. Appl Energy 2024;376:124183. https://doi.org/10.1016/j.apenergy.2024.124183.
[22] Jia J, Wang Y, Lian D. Matlab / simulink based-study on PEM fuel cell and battery hybrid system. Robotics and Vision 2008 10th International Conference on Control, Automation, 2008, p. 2108–13. doi:10.1109/ICARCV.2008.4795856.
[23] Njoya Motapon S, Dessaint L-A, Al-Haddad K. A comparative study of energy management schemes for a fuel-cell hybrid emergency power system of more-electric aircraft. IEEE Trans Ind Electron 2014;61:1320–34. https://doi.org/10.1109/TIE.2013.2257152.
[24] Bassam AM, Phillips AB, Turnock SR, Wilson PA. Development of a multi-scheme energy management strategy for a hybrid fuel cell driven passenger ship. Int J Hydrogen Energy 2017;42:623–35. https://doi.org/10.1016/j.ijhydene.2016.08.209.
[25] Niu L, Xiao L. Optimization of topology and energy management in fuel cell cruise ship hybrid power systems. Intell Mar Technol Syst 2024;2:12. https://doi.org/10.1007/s44295-024-00026-3.
[26] Nazemian A, Boulougouris E, Aung MZ. Simulation of Hybrid Fuel Cell-Battery Propulsion System Scrutinizing Multi-scheme Energy Management for a CTV Boat. In: McNally C, Carroll P, Martinez-Pastor B, Ghosh B, Efthymiou M, Valantasis-Kanellos N, editors. Transport Transitions: Advancing Sustainable and Inclusive Mobility, Cham: Springer Nature Switzerland; 2025, p. 426–31. doi:10.1007/978-3-031-89444-2_62.
[27] Jamma M, Bujlo P, Ulleberg Ø. Intelligent energy management system for hybrid fuel cell/battery powered ships. IEEE Trans Ind Appl 2025;61:8283–96. https://doi.org/10.1109/TIA.2025.3571358.
[28] Afif A, Radenahmad N, Cheok Q, Shams S, Kim JH, Azad AK. Ammonia-fed fuel cells: a comprehensive review. Renew Sustain Energy Rev 2016;60:822–35. https://doi.org/10.1016/j.rser.2016.01.120.
[29] Siddiqui O, Dincer I. Development of a novel hybrid regenerative-electrode ammonia fuel cell and battery system. Energ Conver Manage 2019;181:476–84. https://doi.org/10.1016/j.enconman.2018.12.032.
[30] Hamnett A. Mechanism and electrocatalysis in the direct methanol fuel cell. Catal Today 1997;38:445–57. https://doi.org/10.1016/S0920-5861(97)00054-0.
[31] Motapon SN, Lupien-Bedard A, Dessaint L-A, Fortin-Blanchette H, Al-Haddad K. A generic electrothermal li-ion battery model for rapid evaluation of cell temperature temporal evolution. IEEE Trans Ind Electron 2016;64:998–1008.
[32] Veneri O, Migliardini F, Capasso C, Corbo P. Dynamic behaviour of Li batteries in hydrogen fuel cell power trains. J Power Sources 2011;196:9081–6. https://doi.org/10.1016/j.jpowsour.2011.02.012.
[33] Verstraete D, Lehmkuehler K, Gong A, Harvey JR, Brian G, Palmer JL. Characterisation of a hybrid, fuel-cell-based propulsion system for small unmanned aircraft. J Power Sources 2014;250:204–11. https://doi.org/10.1016/j.jpowsour.2013.11.017.
[34] Andreasen SJ, Ashworth L, Sahlin S, Becker Jensen H-C, Kær SK. Test of hybrid power system for electrical vehicles using a lithium-ion battery pack and a reformed methanol fuel cell range extender. Int J Hydrogen Energy 2014;39:1856–63. https://doi.org/10.1016/j.ijhydene.2013.11.068.
[35] Wilhelm J, Janßen H, Mergel J, Stolten D. Energy storage characterization for a direct methanol fuel cell hybrid system. J Power Sources 2011;196:5299–308. https://doi.org/10.1016/j.jpowsour.2010.09.088.
[36] Kaur D, Singh M, Singh S. 24 - Lithium–sulfur batteries for marine applications. In: Gupta RK, Nguyen TA, Song H, Yasin G, editors. Lithium-Sulfur Batteries, Elsevier; 2022, p. 549–77. doi:10.1016/B978-0-323-91934-0.00019-3.
[37] Bayramoğlu K, Bayraktar M, Seyhan A, Yuksel O. Evaluation of techniques to reduce carbon emissions from ships within the scope of revised greenhouse gas emission targets for 2030, 2040, and 2050. Ocean Eng 2025;334:121605. https://doi.org/10.1016/j.oceaneng.2025.121605.
[38] Seyhan A, Bayraktar M, Yüksel O, Sevgili C. Scenario-based LCOE assessment for bulk carriers within the scope of EU ETS encompassing Carbon Tax, Fuel Prices and GHG Emissions. Clim Change 2026;179:16. https://doi.org/10.1007/s10584-026-04106-7.
[39] Bayraktar M, Yuksel O, Pamik M. An evaluation of methanol engine utilization regarding economic and upcoming regulatory requirements for a container ship. Sustainable Prod Consum 2023;39:345–56.
[40] Kanchiralla FM, Brynolf S, Olsson T, Ellis J, Hansson J, Grahn M. How do variations in ship operation impact the techno-economic feasibility and environmental performance of fossil-free fuels? A life cycle study. Appl Energy 2023:350. https://doi.org/10.1016/j.apenergy.2023.121773.
[41] Xing H, Stuart C, Spence S, Chen H. Alternative fuel options for low carbon maritime transportation: pathways to 2050. J Clean Prod 2021:297. https://doi.org/10.1016/j.jclepro.2021.126651.

[42] Karvounis P, Tsoumpris C, Boulougouris E, Theotokatos G. Recent advances in sustainable and safe marine engine operation with alternative fuels. Front Mech Eng-switzerland 2022:8. https://doi.org/10.3389/fmech.2022.994942.

[43] McKinlay CJ, Turnock SR, Hudson DA. Route to zero emission shipping: Hydrogen, ammonia or methanol? Int J Hydrogen Energy 2021;46:28282–97. https://doi.org/10.1016/j.ijhydene.2021.06.066.

[44] Cheliotis M, Boulougouris E, Trivyza NL, Theotokatos G, Livanos G, Mantalos G, et al. Review on the safe use of ammonia fuel cells in the maritime industry. Energies 2021;14:3023. https://doi.org/10.3390/en14113023.

[45] Yuksel O, Blanco-Davis E, Hitchmough D, Shagar GV, Spiteri A, Di Piazza MC, et al. Integrated Approach to ship electrification using fuel cells and an ammonia decomposition system. J Mar Sci Eng 2025;13:977. https://doi.org/10.3390/jmse13050977.

[46] Di Micco S, Cigolotti V, Mastropasqua L, Brouwer J, Minutillo M. Ammonia-powered ships: Concept design and feasibility assessment of powertrain systems for a sustainable approach in maritime industry. Energy Convers Manage: X 2024;22:100539. https://doi.org/10.1016/j.ecmx.2024.100539.

[47] Di Micco S, Sztrinko P, Cappiello A, Cigolotti V, Minutillo M. Multi-Fuel SOFC system modeling for ship propulsion: comparative performance analysis and feasibility assessment of ammonia, methanol and hydrogen as marine fuels. J Mar Sci Eng 2025;13:1960. https://doi.org/10.3390/jmse13101960.

[48] Liu H, Fan A, Li Y, Bucknall R, Vladimir N. Multi-objective hierarchical energy management strategy for fuel cell/battery hybrid power ships. Appl Energy 2025;379:124981. https://doi.org/10.1016/j.apenergy.2024.124981.

[49] Zhang Z, Guan C, Liu Z. Real-time optimization energy management strategy for fuel cell hybrid ships considering power sources degradation. IEEE Access 2020;8:87046–59. https://doi.org/10.1109/ACCESS.2020.2991519.

[50] Mallouppas G, Ioannou C, Yfantis EA. A review of the latest trends in the use of green ammonia as an energy carrier in maritime industry. Energies 2022;15:doi:10.3390/en15041453.

[51] Li C, Wang Z, Liu H, Guo F, Li C, Xiu X, et al. Energy and configuration management strategy for solid oxide fuel cell/engine/battery hybrid power system with methanol on marine: a case study. Energ Conver Manage 2024;307:118355. https://doi.org/10.1016/j.enconman.2024.118355.

[52] Sun Y, Shang Q, Jiang W. Equivalent minimum hydrogen consumption of fuzzy control-based fuel cells: exploration of energy management strategies for ships. Batteries 2024;10:66. https://doi.org/10.3390/batteries10020066.

[53] Dall'Armi C, Micheli D, Taccani R. Comparison of different plant layouts and fuel storage solutions for fuel cells utilization on a small ferry. Int J Hydrogen Energy 2021;46:13878–97. https://doi.org/10.1016/j.ijhydene.2021.02.138.

[54] Kolodziejski M, Michalska-Pozoga I. Battery energy storage systems in ships' hybrid/electric propulsion systems. Energies 2023;16:1122. https://doi.org/10.3390/en16031122.